Hindawi
International Journal of Antennas and Propagation
Volume 2021, Article ID 9955502, 10 pages
https://doi.org/10.1155/2021/9955502

Research Article

A Millimeter-Wave Wideband Circularly Polarized Planar Spiral Antenna Array with Unequal Amplitude Feeding Network

Huakang Chen,[1] **Yu Shao**,[1] **Zhangjian He**,[1] **Changhong Zhang**,[1] **and Zhizhong Zhang**[2]

[1]*School of Communication and Information Engineering, Chongqing University of Posts and Telecommunications, Chongqing 400065, China*
[2]*School of Electronic and Information Engineering, Nanjing University of Information Science and Technology, Nanjing 210044, China*

Correspondence should be addressed to Yu Shao; shaoyu@cqupt.edu.cn

Received 18 March 2021; Revised 31 May 2021; Accepted 19 July 2021; Published 27 July 2021

Academic Editor: María Elena de Cos Gómez

Copyright © 2021 Huakang Chen et al. This is an open access article distributed under the Creative Commons Attribution License, which permits unrestricted use, distribution, and reproduction in any medium, provided the original work is properly cited.

A 2 × 2 wideband circularly polarized (CP) antenna array operating at millimeter wave (mmWave) band is presented. The array element is a wideband CP Archimedean spiral radiator with special-shaped ring slot. The elements are fed by an unequal amplitude (UA) feeding network based on a microstrip line (MSL) power divider. The side lobe level is improved by this UA feeding network. In addition, a cross slot is employed to isolate the elements for decoupling. A prototype is fabricated, and the measured results show that the proposed array achieves an impedance bandwidth (IBW) of 6.31 GHz (22.5% referring to 28 GHz) and an axial ratio bandwidth (ARBW) of 7.32 GHz (26.1% referring to 28 GHz). The peak gain of the proposed array is 11.3 dBic, and the gain is greater than 9.3 dBic within the whole desired band (from 25 GHz to 31 GHz). The proposed array consists of only one substrate layer and can be built by the conventional printed circuit board technology. Attributed to the characteristics of wide bandwidth, simple structure, low profile, and low cost, the proposed antenna array has a great potential in mmWave wireless communications.

1. Introduction

With the rapid popularization of the fifth-generation (5G) wireless communication technology and the growth of wireless data traffic, millimeter wave (mmWave) communication has become one of the most attractive technologies in the 5G mobile communication system [1]. Antennas are usually arranged into arrays for high gain to compensate the large path loss in mmWave band. Moreover, since the circularly polarized (CP) antenna can suppress multipath and prevent rain and fog interference, the mmWave CP arrays with wide bandwidth has been widely concerned by academia and industry.

In recent decades, many researchers have studied the mmWave wideband CP array. One of the most widely used techniques to realize CP array is the sequentially rotated phase (SRP) feeding. In a typical SRP feeding array, four single-feeding radiation elements are rotated clockwise or anticlockwise, and the elements are fed with equal amplitude and 90 degrees phase difference. The SRP feeding technique is beneficial to improve the bandwidth and polarization purity of CP array. The reported structures of SRP feeding network in the mmWave band can be divided into three categories: (1) microstrip line (MSL) SRP feeding network [2–5], (2) substrate-integrated waveguide (SIW) SRP feeding network [6–9], and (3) grounded coplanar waveguide (GCPW) SRP feeding network [10, 11]. A 61 GHz beam steering antenna with left-handed linear polarized polarization (LHCP) fed by MSL clockwise SRP network was presented in [2]. A 4 × 4 wideband CP cross-aperture-coupled stacked array operating at 60 GHz and a 4 × 4 CP crossed slot with parasitic patch array operating at 28 GHz were presented in [3, 4], respectively. A 4 × 4 mmWave wideband CP microstrip array with right-handed circular polarization (RHCP) was proposed in [5], which consisted of an edge-coupled parasitic patch structure and a novel series

anticlockwise SRP feeding network. A low-profile cavity-backed slot CP 2×2 array and a 2×2 wideband RHCP diamond ring slot antenna array at the X-band were realized by employing the SIW SRP feeding network structure in [6, 7], respectively. Jianfeng Zhu presented a dual CP planar aperture array operating at 60 GHz fed through two input ports connecting with the SRP feeding network [8]. A 45 GHz wideband CP array using inclined slot in SIW was developed by using SRP feeding network in [9]. Moreover, an mmWave CP differentially fed dipole array [10] and an mmWave CP array with the truncated-corner square patch as radiation element [11] were realized by employing GCPW SRP feeding network and substrate-integrated gap waveguide (SIGW) SRP feeding network, respectively. The SRP feeding can enhance the axial ratio bandwidth (ARBW) of CP array, even if the element has a narrow ARBW. However, the above designs have shown that the structure of SRP feeding network and the placement of antenna elements are complex.

Another feeding method to realize wideband CP array is the full-corporate (FC) feeding technique based on the power divider. In FC feeding network, the elements are excited with equal amplitude and equal phase. Ming Du presented wideband CP patch array are fed by MSL FC feeding network with low-temperature cofired ceramic (LTCC) technology in [12]. A wideband CP 4×4 mmWave array operating at 45 GHz was realized by utilizing MSL FC feeding network to excite the microstrip elements in [13]. The SIW technique has also been applied in FC feeding network. In [14], a 60 GHz 2×2 planar array with RHCP was fed by SIW FC feeding network. Long Zhang presented an mmWave wideband CP 4×4 antenna array which consisted of SIW FC feeding network and S-dipole elements in [15], and this design was improved in [16], in which a 8×8 array with S-dipole radiation elements was presented. A 16×16 and a 8×8 high-gain wideband CP array operating at 60 GHz were developed by using magneto-electric dipoles in [17, 18], respectively, in which the radiation elements were excited by SIW FC feeding network. Yue Zhao proposed a high-gain CP scalable array operating at 60 GHz [19], and this array consisted of cross-slot-coupled patch elements fed by a SIW FC feeding network. FC feeding network may suffer from high side-lobe level, and unequal feeding network can alleviate this problem. An mmWave low side-lobe linearly polarized SIW array was designed by using wideband unequal feeding network [20]. However, wideband CP arrays fed by unequal feeding network are seldom reported. Moreover, most of the aforementioned designs contain multiple substrate layers which increase complexity in fabrication.

In this paper, a 2×2 mmWave wideband CP antenna array is proposed. This array has a single layer structure, and it is fed by a parallel feeding network with equal phase unequal amplitude (UA) which can improve the side-lobe level. The array operates at 28 GHz with the impedance bandwidth (IBW) of 22.5% and ARBW of 26.1%. The peak gain of this array is 11.3 dBic. A prototype is fabricated with simple printed circuit board (PCB) technique. The simulated and measured results agree very well. The proposed mmWave wideband CP array has the advantages of simple structure, low profile, and low cost, which make it have great application prospects in the field of mmWave communications in the future.

The contents of this paper are arranged as follows. The design procedure of the proposed array is presented in Section 2. The verification and measured results are discussed in Section 3. Section 4 is a conclusion of the whole paper.

2. Antenna Design

The geometry of the proposed mmWave wideband CP array is shown in Figure 1. This antenna array is simply constructed on single substrate with two copper layers. The substrate is Rogers RT/Duroid 5880 with a thickness of 0.254 mm, dielectric constant of 2.2, and loss tangent of 0.0009. The wideband CP radiating element of the array consists of a planar Archimedean spiral on the top layer of the substrate and a special-shaped ring slot etched on the bottom layer. Four of these radiating elements are arranged as a 2×2 array. Besides, a cross slot with a width of W_s is introduced into the bottom copper layer of the array to isolate each radiating element for decoupling. A MSL feeding network based on the unequal power divider is employed to feed the array, and this feeding network feeds each element with the equal phase but UA. A GCPW structure connects to the MSL feeding network to mount the coaxial connector for measurement. The diameters of the connector mounting holes on the two sides of GCPW are 2 mm. All the simulations on the proposed array are performed by Computer Simulation Technology (CST) Studio Suite 2019.

2.1. Radiating Element. Figure 2 shows the top view and bottom view of the proposed radiating element. This radiating element is based on our previous work [21], in which a planar Archimedean spiral on the top layer and a special-shaped ring slot on the bottom layer are used to generate annular currents for CP radiation. CP radiation can be generated by both archimedean spiral and special-shaped ring slot, and these two radiators couple together to significantly improve the ARBW and radiation pattern. The ARBW of the element achieves 8.35 GHz from 23.85 GHz to 32.2 GHz (29.82% referring to 28 GHz), which is beneficial to build wideband CP array. The gain of the element is 6.49 dBic at 28 GHz and is larger than 5.2 dBic within the desired frequency band. In this letter, four of such radiating elements are employed to construct a 2×2 antenna array. The dimensions of the radiating element are shown in Table 1.

2.2. Array Design. Four of the radiating elements are arranged into a 2×2 array, and the distance between adjacent radiating elements is denoted as D_e in Figure 1. D_e is a critical parameter which impacts the radiating performance of the array greatly. Large D_e can lead to grating lobe, while strong mutual coupling may occur between elements if D_e is

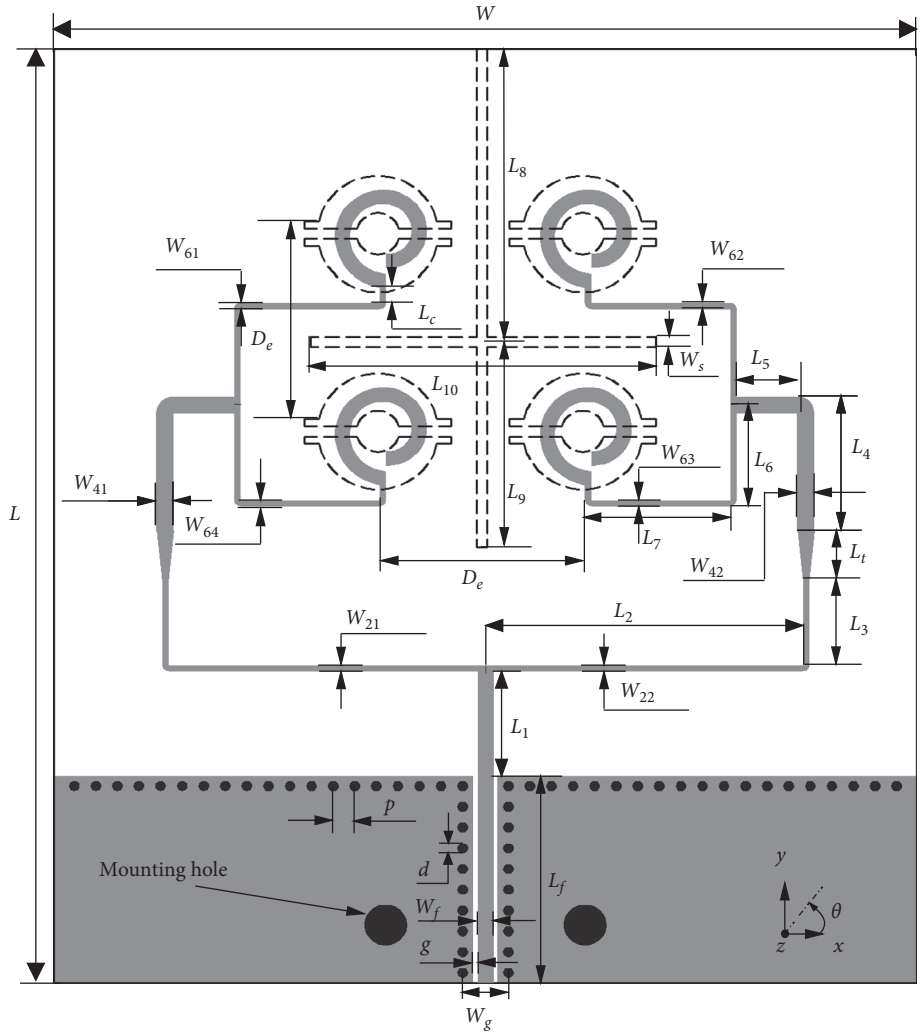

Figure 1: Geometry of the proposed mmWave wideband CP antenna array.

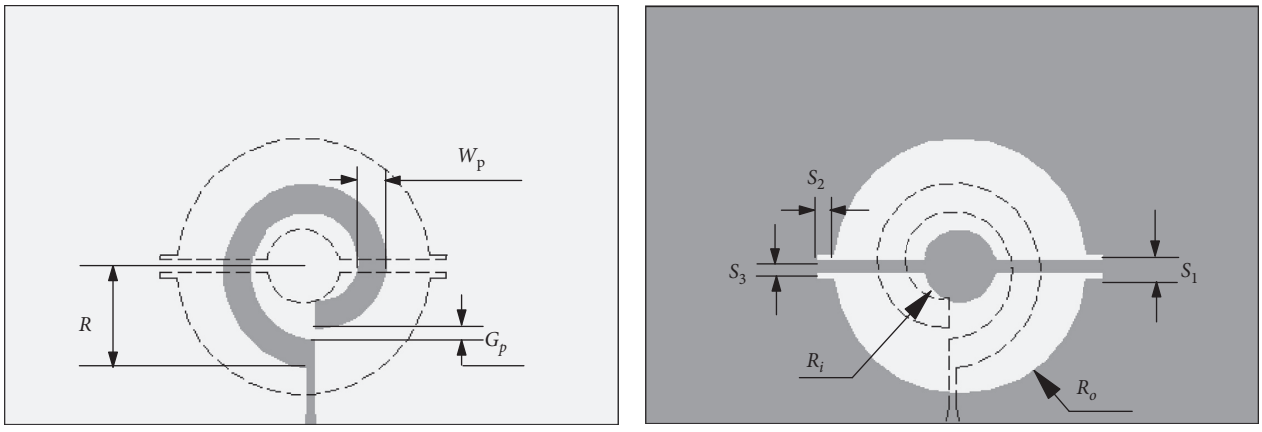

Figure 2: Detailed views of the proposed radiating element: (a) top view and (b) bottom view.

too small, which will deteriorate the overall performance of the array. In this work, D_e is set to be $0.6\lambda_0$ to $0.8\lambda_0$, where λ_0 is the free space wavelength at the central frequency of 28 GHz which is about 10.7 mm. Figure 3 shows the reflection coefficient S_{11} and axial ratio (AR) varying against D_e. It can be seen that wider IBW and ARBW can be

Table 1: Parameters of the proposed radiating element.

Parameter	R	Wp	Gp	Ro	Ri	$S1$	$S2$	$S3$
Value (mm)	2.63	1	0.17	2.7	1	0.6	0.6	0.2

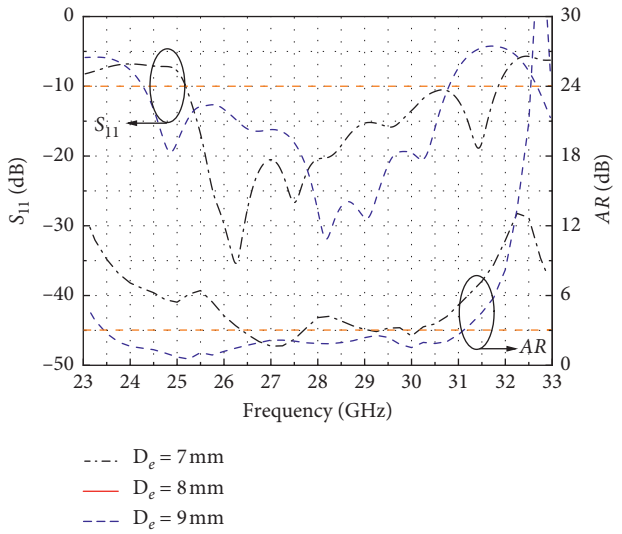

Figure 3: Variations of S_{11} and AR with De.

obtained when D_e is set to be 8 mm. Meanwhile, a cross slot with width of W_s is introduced into the bottom layer of the radiating elements to reduce mutual coupling [22], whose lengths are denoted as L_8, L_9, and L_{10} in Figure 1.

The proposed antenna array is fed by a parallel network consists of a four-way MSL power divider and a GCPW transmission line, as shown in Figure 1. The connector is mounted on the edge of GCPW for measurement. For characteristic impedance of 50 Ω, the feed line width W_f of GCPW and MSL is set to be 0.74 mm, and the gap width g in GCPW structure is set to be 0.2 mm. The four-way power divider is composed of a two-way MSL power divider in the first stage and two parallel two-way MSL power dividers in the second stage. A quarter wavelength impedance transformer with a length of L_t is applied to connect the two stages of the power divider. The wavelength λ_g in the MSL is figured out to be 7.22 mm at 28 GHz, so the value of L_t is set as 1.8 mm. The width of the impedance transformer is tapered to enhance the bandwidth of impedance. The lengths of remaining MSLs are denoted as L_1, L_2, L_3, L_4, L_5, L_6, and L_7.

The array elements are fed by the FC power divider with equal amplitude and phase at first [23]. In order to carry out comparative analysis, the results of the proposed array are simulated with and without the FC power divider. Figure 4 shows the simulated gain and AR of the proposed array with and without the FC power divider. It is obvious that this array without a power divider has wider ARBW and higher gains than those of the one with the FC power divider.

The power divider not only affects the bandwidth of the proposed array but also affects its radiation patterns. The comparisons of simulated radiation patterns of the proposed array with and without power divider at 25, 28, and 31 GHz

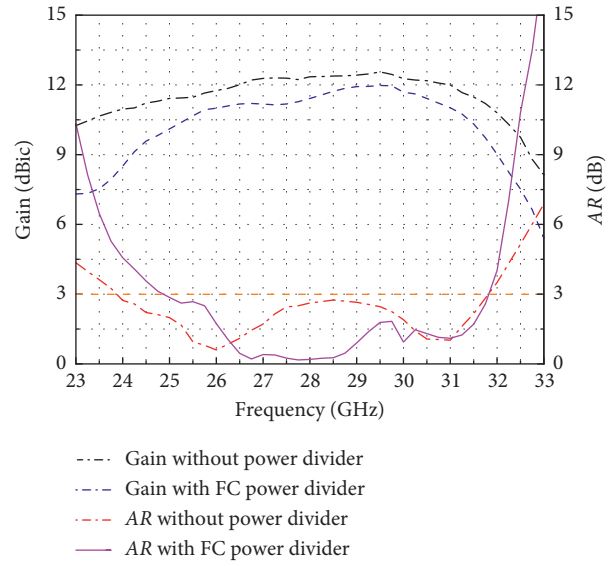

Figure 4: Simulated gain and AR of the proposed array with and without the FC power divider.

are shown in Figures 5(a)–5(c), respectively. The red solid lines in Figures 5(a)–5(c) show the side lobe levels of the proposed array are increased by introducing the FC power divider. Especially, the side lobe in 60 degree at 31 GHz is only −5 dB lower than the main lobe level.

To suppress the side lobe, an unequal feeding network is designed to feed each element with equal phase but UA. The characteristic impedances assigned to each microstrip line of FC feeding network and UA feeding network are shown in Figures 6(a) and 6(b), respectively. With the value of characteristic impedance, the widths of each MSL which are denoted as W_{21}, W_{22}, W_{41}, W_{42}, W_{61}, W_{62}, W_{63}, and W_{64} in Figure 1 can be determined by the following equation:

$$Z_0 = \frac{87}{\sqrt{\varepsilon_r + 1.41}} \ln\left(\frac{5.98h}{0.8W + t}\right), \quad (1)$$

where Z_0 is the characteristic impedance, ε_r is the relative dielectric constant of the substrate, h is the thickness of the substrate, W is the width of the microstrip line, and t is the thickness of the copper layer which is 35 μm here.

The simulated magnitude and phase of the S-parameters of the proposed four-way FC power divider and UA power divider are shown in Figures 7(a) and 7(b), respectively. In Figure 7(a), the magnitude of transmission coefficient at each of the four output ports is around −7 dB, which is slightly lower than the theoretical value of −6 dB for a four-ways FC power divider due to the loss of MSL. The phases are exactly the same at each output port for the FC power divider. In Figure 7(b), the magnitudes of transmission coefficients at the four output ports are different, ranging from −5.9 dB to −8.9 dB within the desired band from 25 GHz to 31 GHz. Since the UA feeding network is not symmetry, the phase deviates a little from each other at the output ports. This deviation is less than 20 degree within the desired band, for simplicity no extra phase compensation is applied.

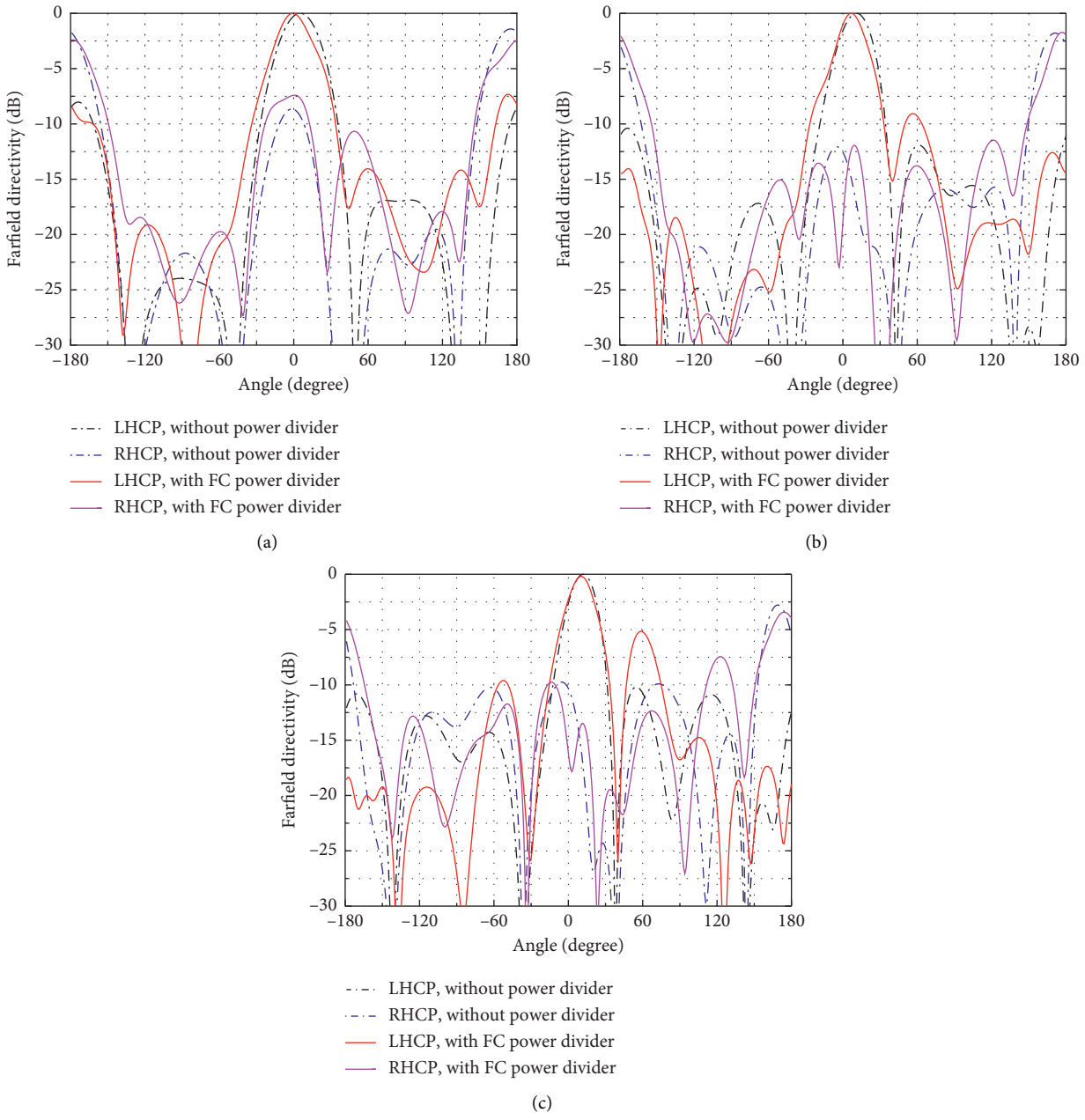

Figure 5: Simulated radiation patterns of the proposed array with and without a power divider: (a) radiation patterns at 25 GHz, (b) radiation patterns at 28 GHz, and (c) radiation patterns at 31 GHz.

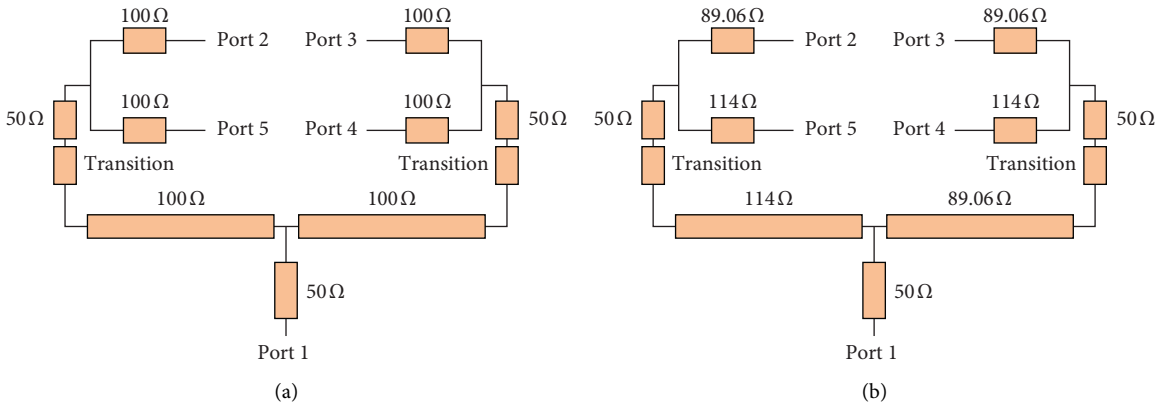

Figure 6: Schematic of four-way feeding network: (a) FC power divider; (b) UA power divider.

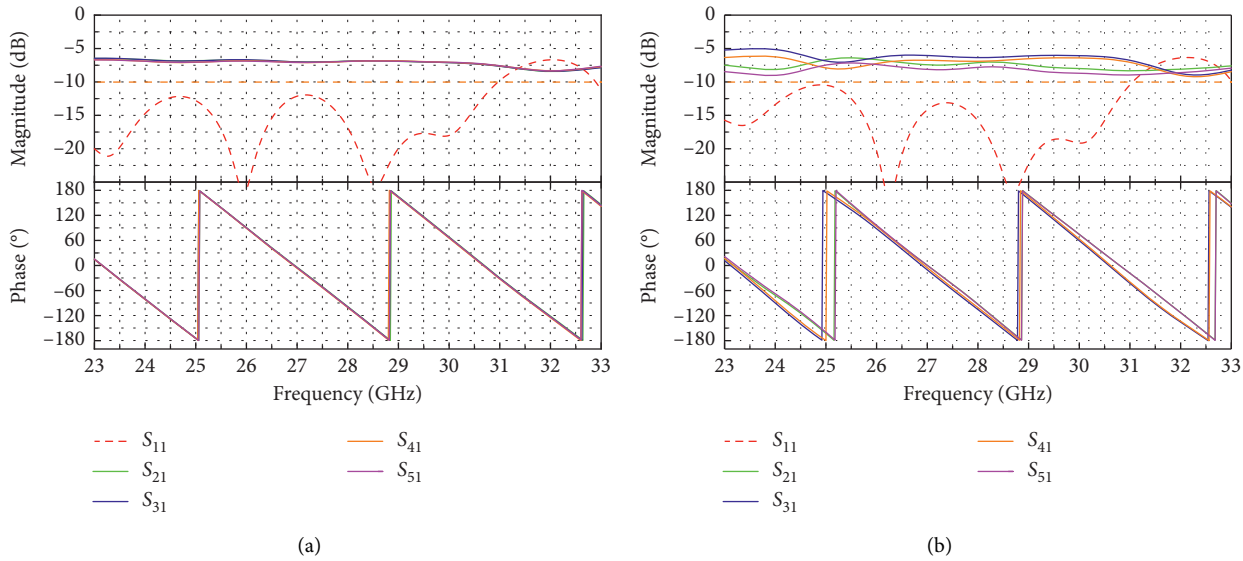

Figure 7: Simulated S-parameters of four-way power divider: (a) FC power divider; (b) UA power divider.

The simulated radiation patterns of the proposed array at 31 GHz with FC feeding network and UA feeding network are shown in Figure 8. There is a large side lobe at 60 degree in the radiation pattern, and the side lobe level is about −5 dB when using the FC feeding network (black dot dash line in Figure 8). In comparison, the side lobe level is improved to be -9 dB for UA feeding network (red solid line in Figure 8). So, the UA feeding network is employed in this letter, and its dimensions are listed in Table 2.

3. Experimental Results

A prototype is fabricated to verify the proposed 2 × 2 mmWave wideband CP array based on the parameters shown in Tables 1 and 2. The prototype is fabricated by using the printed circuit board (PCB) technology which has a low cost. The array is connected with a 50 Ω southwest microwave 2.92 mm end launch connector for measurement. Figure 9 shows the top view and back view of the fabricated prototype, as well as its measurement scene in an anechoic chamber. The antenna under test (AUT) transmits CP waves to the auxiliary antenna (linearly polarized horn antenna). A controlled polarizer is connected with the auxiliary antenna so that the auxiliary antenna can be rotated from 0° to 360°. The maximum received power by the auxiliary antenna is recorded as P_{max}, and the minimum received power is recorded as P_{min} (specify: P_{max} and P_{min} in dBm). With these results, AR of the proposed array can be obtained simply by the following equation (specify: AR in dB):

$$\mathrm{AR} = P_{max} - P_{min}. \quad (2)$$

Figure 10 shows the simulated and measured reflection coefficients (S_{11}) and AR of the proposed array. The red dotted line shows that the bandwidth for S_{11} lower than -10 dB is from 25.01 GHz to 31.32 GHz, which means the IBW of the proposed array is about 6.31 GHz (22.5% referring to 28 GHz). As shown, the measured ARBW, within which AR is lower than 3 dB, is from 24.47 GHz to 31.79 GHz. So, the measured ARBW is about 7.32 GHz (26.1% referring to 28 GHz). The simulated results generally agree with the measured results.

The simulated and measured gains of the proposed array are illustrated in Figure 11. It shows that the measured peak gain is 11.3 dBic at 26.5 GHz, and the variations of gains are smaller than 2 dB within the operating frequency band from 25 GHz to 31 GHz. The measured gain is approximately 1 dB lower than the simulated gain, which may be caused by connector loss and inaccuracies of substrate parameters in simulation. The simulated radiation efficiency of the proposed array is 94% at 28 GHz and greater than 88% within the desired band.

Based on the coordinate system in Figure 1, the simulated and measured normalized radiation patterns at the 25 GHz, 28 GHz, and 31 GHz in the *xoz* plane and the *yoz* plane are depicted in Figures 12(a)–12(c) and 13(a)–13(c), respectively. The measured results agree well with the simulated ones. It can be observed that the primary polarization of the proposed array is LHCP at the top and RHCP at the bottom. The radiation patterns are similar within the operating band except the direction of maximum radiation in the *xoz* plane tiled from *z*-axis as the frequency increases. For example, the maximum radiation at 31 GHz points to the angle of 14° from *z*-axis, as shown in Figure 12(c) which is due to the asymmetry of the planar spiral.

Table 3 shows the comparisons between the proposed array and some similar mmWave wideband CP arrays. The proposed array achieves the bandwidth and gain comparable to other similar designs by applying an UA feeding network, and it can be fabricated with low cost PCB technology. Since the array in this work has only one substrate layer and one feeding port, its structure is much simpler than many other designs, and it is easy to be integrated into a circuit board.

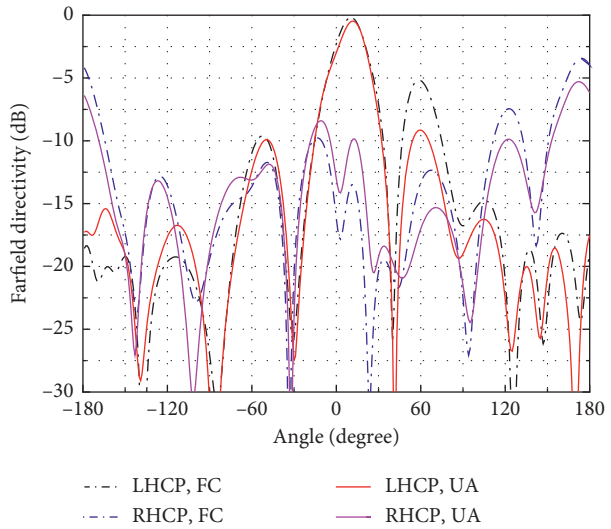

Figure 8: Simulated radiation patterns at 31 GHz of the proposed array with different feeding networks.

Table 2: Parameters of the proposed array.

Parameter	L	W	L_f	W_f	L_t	W_g	L_c	W_s
Value (mm)	45	40	10	0.74	1.8	2.2	0.5	0.2
Parameter	W_{21}	W_{22}	W_{41}	W_{42}	W_{61}	W_{62}	W_{63}	W_{64}
Value (mm)	0.13	0.25	0.74	0.74	0.25	0.25	0.13	0.13
Parameter	L_1	L_2	L_3	L_4	L_5	L_6	L_7	L_8
Value (mm)	5	13.2	4	6.5	2.8	4	5.97	15.03
Parameter	L_9	L_{10}	D_e	d	g	p		
Value (mm)	8.97	16	8	0.5	0.2	1		

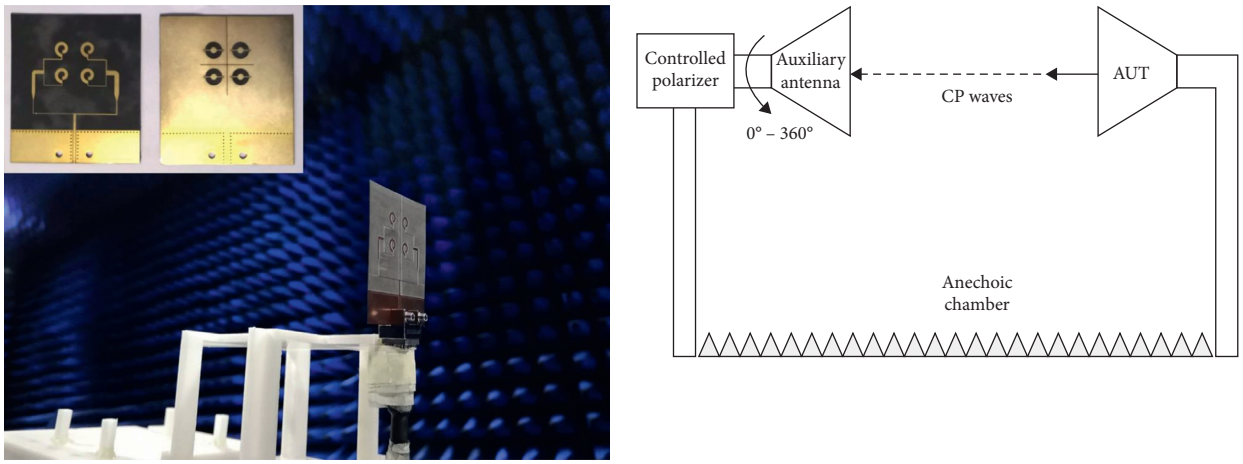

(a) (b)

Figure 9: Photos of the top view, the back view, and the measurement system for the fabricated array.

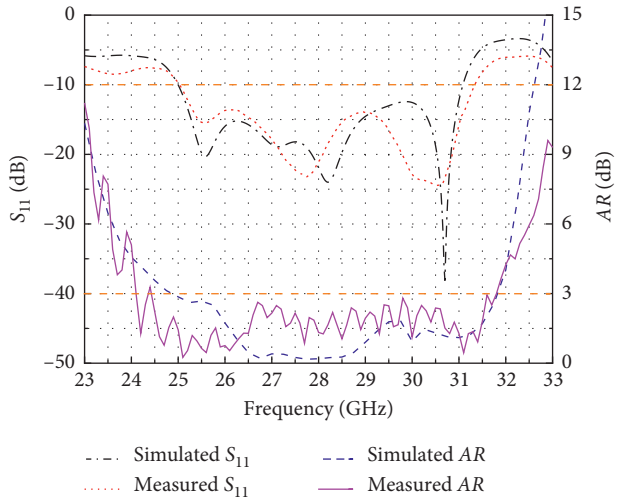

Figure 10: Reflection coefficients and axial ratios of the proposed array.

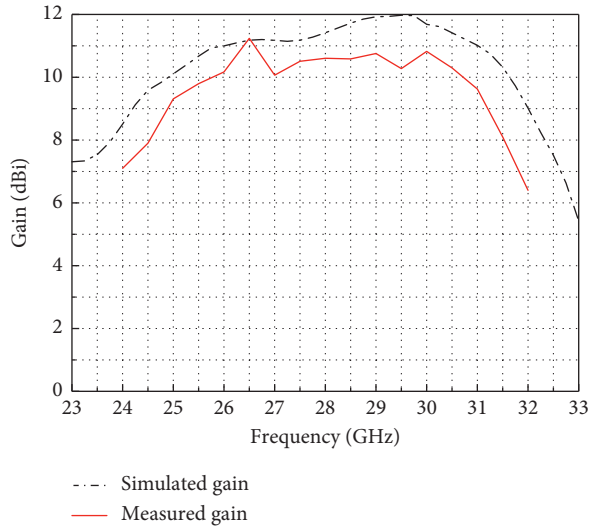

Figure 11: Simulated and measured gains of the proposed array.

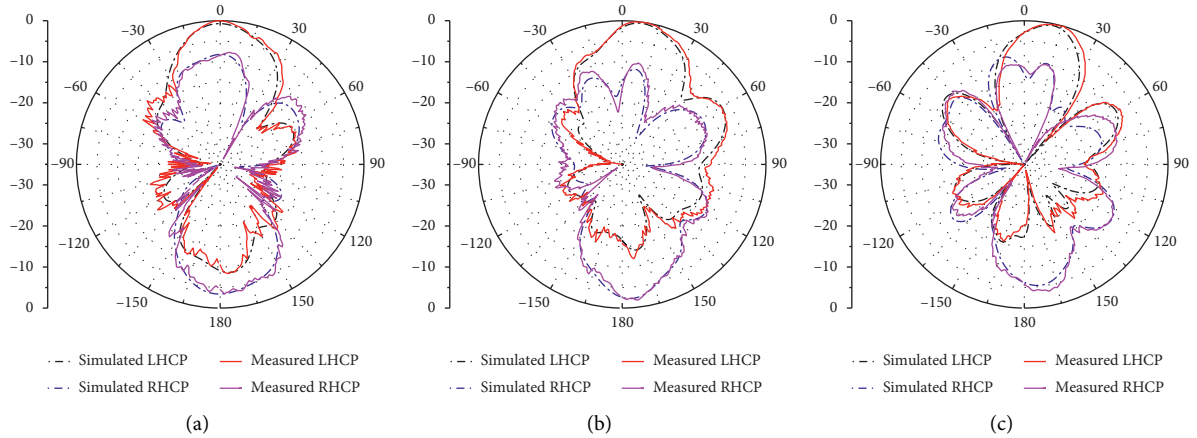

Figure 12: Measured and simulated radiation patterns of the proposed array in the *xoz* plane: (a) radiation patterns at 25 GHz, (b) radiation patterns at 28 GHz, and (c) radiation patterns at 31 GHz.

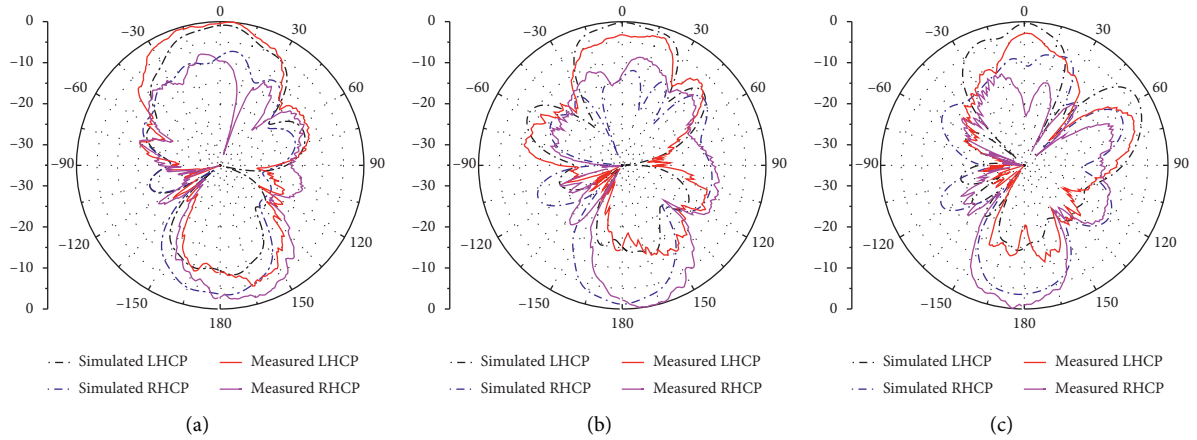

Figure 13: Measured and simulated radiation patterns of the proposed array in the *yoz* plane: (a) radiation patterns at 25 GHz, (b) radiation patterns at 28 GHz, and (c) radiation patterns at 31 GHz.

Table 3: Comparisons to reported 2 × 2 mmWave wideband CP antenna arrays.

Ref.	Fre. (GHz)	Feed type	IBW (%)	ARBW (%)	Structure	Gain (dBic)
[2]	61	SRP in MSL	16	5.0	Single feed, 1 layer-3D	14
[6]	28	SRP in SIW	23.3	7.7	Single feed, 2 layers-PCB	10.8
[7]	10.3	SRP in SIW	19.2	14.1	Single feed, 2 layers-PCB	13.48
[9]	45.5	SRP in SIW	14.7	14.7	Dual feed, 2 layers-PCB	10.5
[10]	62.2	SRP in GCPW	32.2	32.2	Dual feed, 1 layer-PCB	11.8
[11]	26	SRP in SIGW	25.6	19.0	Single feed, 5 layers-PCB	11.53
[12]	35	FC in MSL	29.6	26.0	Single feed, 14 layers-LTCC	9.3
[14]	60	FC in SIW	6.6	6.8	Single feed, 2 layers-PCB	12.5
This work	28	UA in MSL	22.5	26.1	Single feed, 1 layer-PCB	11.3

4. Conclusions

A low-profile mmWave wideband CP 2 × 2 antenna array is proposed. A four-way UA feeding network based on the MSL power divider is applied to feed each planar Archimedean spiral radiator. The UA feeding network leads to about 4 dB reduction in the side lobe level compared with the FC feeding network. A cross slot is introduced into the bottom layer to isolate radiating elements for decoupling. A prototype is fabricated with PCB technology, and its performances are measured and evaluated. The measured results show good agreement with the simulated results. The proposed array obtains an IBW of 22.5% and ARBW of 26.1% referring to 28 GHz. The measured peak gain of the proposed array is about 11.3 dBic. The characteristics of wideband, simple structure, low profile, and low cost make the proposed array as a potential candidate in mmWave communication applications.

Data Availability

No data were used to support this study.

Conflicts of Interest

The authors declare that there are no conflicts of interest regarding the publication of this paper.

Acknowledgments

This work was supported in part by the National Natural Science Foundation of China, under Grant 61701061, and 61801070, and Natural Science Foundation of Chongqing, under Grant cstc2019jcyj-msxmX0606.

References

[1] J. Zhang, X. Ge, Q. Li, M. Guizani, and Y. Zhang, "5G millimeter-wave antenna array: design and challenges," *IEEE Wireless Communications*, vol. 24, no. 2, pp. 106–112, 2017.

[2] K.-C. Huang and Z. Wang, "Millimeter-wave circular polarized beam-steering antenna array for gigabit wireless communications," *IEEE Transactions on Antennas and Propagation*, vol. 54, no. 2, pp. 743–746, 2006.

[3] L. Wang, Y. X. Guo, and W. Wu, "Wideband 60 GHz circularly polarised stacked patch antenna array in low-temperature co-fired ceramic technology," *IET Microwaves, Antennas & Propagation*, vol. 9, no. 5, pp. 436–445, 2015.

[4] J. Wu, Y. J. Cheng, and Y. Fan, "Millimeter-wave wideband high-efficiency circularly polarized planar array antenna," *IEEE Transactions on Antennas and Propagation*, vol. 64, no. 2, pp. 535–542, 2016.

[5] B. Lee and Y. Yoon, "Low-profile, low-cost, broadband millimeter-wave antenna array for high-data-rate WPAN systems," *IEEE Antennas and Wireless Propagation Letters*, vol. 16, pp. 1957–1960, 2017.

[6] Q. Wu, H. Wang, C. Yu, and W. Hong, "Low-profile circularly polarized cavity-backed antennas using SIW techniques," *IEEE Transactions on Antennas and Propagation*, vol. 64, no. 7, pp. 2832–2839, 2016.

[7] F. F. Fan, Z. H. Yan, and W. Wang, "Wideband circularly polarized SIW antenna array that uses sequential rotation feeding," *International Journal of Antennas and Propagation*, vol. 2014, Article ID 534539, 8 pages, 2014.

[8] J. Zhu, S. Liao, Y. Yang, S. Li, and Q. Xue, "60 GHz dual-circularly polarized planar aperture antenna and array," *IEEE Transactions on Antennas and Propagation*, vol. 66, no. 2, pp. 1014–1019, 2018.

[9] Y. Zhang, W. Hong, and R. Mittra, "45 GHz wideband circularly polarized planar antenna array using inclined slots in modified short-circuited SIW," *IEEE Transactions on Antennas and Propagation*, vol. 67, no. 3, pp. 1669–1680, 2019.

[10] X. Ruan and C. H. Chan, "A circularly polarized differentially fed transmission-line-excited magnetoelectric dipole antenna array for 5G applications," *IEEE Transactions on Antennas and Propagation*, vol. 67, no. 3, pp. 2002–2007, 2019.

[11] C. Ma, Z.-H. Ma, and X. Zhang, "Millimeter-wave circularly polarized array antenna using substrate-integrated gap waveguide sequentially rotating phase feed," *IEEE Antennas and Wireless Propagation Letters*, vol. 18, no. 6, pp. 1124–1128, 2019.

[12] M. Du, Y. Dong, J. Xu, and X. Ding, "35 GHz wideband circularly polarized patch array on LTCC," *IEEE Transactions on Antennas and Propagation*, vol. 65, no. 6, pp. 3235–3240, 2017.

[13] Z. Gan, Z.-H. Tu, Z.-M. Xie, Q.-X. Chu, and Y. Yao, "Compact wideband circularly polarized microstrip antenna array for 45 GHz application," *IEEE Transactions on Antennas and Propagation*, vol. 66, no. 11, pp. 6388–6392, 2018.

[14] A. B. Guntupalli and K. Ke Wu, "60 GHz circularly polarized antenna array made in low-cost fabrication process," *IEEE Antennas and Wireless Propagation Letters*, vol. 13, pp. 864–867, 2014.

[15] L. Zhang, Y. He, S. Wong et al., "Millimeter-wave wideband circularly polarized antenna array using SIW-fed S-dipole elements," in *Proceedings of the International Symposium on Antennas and Propagation and USNC-URSI Radio Science Meeting*, pp. 1231-1232, Atlanta, GA, USA, 2019.

[16] L. Zhang, K. Wu, S.-W. Wong et al., "Wideband high-efficiency circularly polarized SIW-fed S-dipole array for millimeter-wave applications," *IEEE Transactions on Antennas and Propagation*, vol. 68, no. 3, pp. 2422–2427, 2020.

[17] Y. Li, J. Wang, J. Wang et al., "Millimeter-wave high-gain wideband circularly polarized antenna array by employing aperture-coupled magneto-electric dipoles," in *Proceedings of the International Symposium on Antennas and Propagation*, pp. 656-657, Okinawa, Japan, 2016.

[18] Y. Li and K.-M. Luk, "A 60 GHz wideband circularly polarized aperture-coupled magneto-electric dipole antenna array," *IEEE Transactions on Antennas and Propagation*, vol. 64, no. 4, pp. 1325–1333, 2016.

[19] Y. Zhao and K.-M. Luk, "Dual circular-polarized SIW-fed high-gain scalable antenna array for 60 GHz applications," *IEEE Transactions on Antennas and Propagation*, vol. 66, no. 3, pp. 1288–1298, 2018.

[20] S.-J. Park, D.-H. Shin, and S.-O. Park, "Low side-lobe substrate-integrated-waveguide antenna array using broadband unequal feeding network for millimeter-wave handset device," *IEEE Transactions on Antennas and Propagation*, vol. 64, no. 3, pp. 923–932, 2016.

[21] H. Chen, Y. Shao, Y. Zhang, C. Zhang, and Z. Zhang, "A low-profile broadband circularly polarized mm wave antenna with special-shaped ring slot," *IEEE Antennas and Wireless Propagation Letters*, vol. 18, no. 7, pp. 1492–1496, 2019.

[22] J. OuYang, F. Yang, and Z. M. Wang, "Reducing mutual coupling of closely spaced microstrip MIMO antennas for WLAN application," *IEEE Antennas and Wireless Propagation Letters*, vol. 10, pp. 310–313, 2011.

[23] H. K. Chen, Y. Shao, Y. J. Zhang et al., "Low-profile millimeter-wave wideband circularly polarized spiral antenna array," in *Proceedings of the European Conference on Antennas and Propagation (EuCAP)*, pp. 1–4, Copenhagen, Denmark, 2020.